CHAPTER VII
ETHYLENE EPOXIDATION IN AN AC DIELECTRIC BARRIER DISCHARGE JET SYSTEM

(Being Prepared for International Journal of Chemical Engineering Journal)

7.1 Abstract

In this work, the ethylene epoxidation was investigated in a low-temperature dielectric barrier discharge (DBD) jet system under high flow rate and O_2-lean conditions. The C_2H_4 stream was directly injected at the end of the plasma zone in order to reduce C_2H_4 cracking and other reactions, while the O_2 balanced with argon was fed through the plasma zone for generating active oxygen species. The effects of various operating parameters, such as total feed flow rate, O_2/C_2H_4 feed molar ratio, applied voltage, input frequency, and inner electrode position on the ethylene epoxidation activity, were investigated to achieve the optimum operating conditions for this new DBD jet system. The highest EO selectivity and yield, as well as the lowest power consumption were obtained at a total feed flow rate of 1,625 cm^3/min (corresponding to a residence time of 0.0229 s), an O_2/C_2H_4 feed molar ratio of 0.25:1, an applied voltage of 9 kV, an input frequency of 300 Hz, and an inner electrode position of 0.3 mm.

Keywords: Epoxidation; Ethylene oxide; Dielectric barrier discharge; Atmospheric plasma jet

7.2 Introduction

Ethylene epoxidation is very important in the petrochemical industry. Ethylene oxide (C_2H_4O, EO)— a desired product from the partial oxidation of ethylene, so-called ethylene epoxidation— is increasingly demanded as a chemical feedstock for various downstream processes to produce several useful derivatives such as antifreeze agents, automotive coolants, polyesters, detergents, etc [1]. In

addition, it is also used as a sterilant for foodstuffs, in medical equipment and supplies, and as a fumigant in agricultural products [2].

Commercially, the catalytic processes using silver-based catalysts, especially low-surface-area (LSA) α-alumina-supported silver catalyst (Ag/(LSA) α-Al_2O_3) are used in this reaction. Alkali and transition metals such as cesium (Cs), copper (Cu), rhenium (Re), and gold (Au) were reported to significantly enhance EO selectivity [3-13]. Moreover, a small amount of chloride adding to reactant gases also improved the ethylene epoxidation activity [10,14-16]. Although the catalytic processes exhibit high EO selectivity, high temperature is required to operate the catalytic processes, leading to high energy consumption. The high-temperature catalytic problems, including catalytic deactivation directly lowers process efficiency. Therefore, there are many attempts to research a new technique in order to solve these limitations and to provide a better ethylene epoxidation performance.

Non-thermal plasma, i.e. dielectric barrier discharge (DBD), corona discharge, glow discharge, microwave, etc., is considered to be a promising technique because of its various applications [17-25]. Moreover, this technique has a valuable characteristic that it can generate highly energetic electrons, while the bulk gas temperature is comparatively low (at room temperature or slightly higher) [26,27]. These imply that the non-thermal plasma can be operated under atmospheric pressure and ambient temperature, resulting in low energy consumption, as well as it can overcome the above mentioned catalyst problems at high-temperature operation.

Recently, the ethylene epoxidation has been investigated in different non-thermal plasma reactors— a corona discharge reactor, a parallel and cylindrical DBD reactor [28-31]. The cylindrical DBD was reported to exhibit the best performance in terms of the highest EO selectivity with the lowest power consumption, as compared to the other plasma systems. In spite of high EO selectivity, the ethylene conversion was still low and other products were produced in the plasma zone. Therefore, a cylindrical DBD reactor is necessary to be redesigned in order to improve ethylene epoxidation performance.

Atmospheric plasma jets— dielectric barrier discharge (DBD) jets— have currently been great of interest in current low-temperature plasma research [32]. The plasma jet reactors can generate highly reactive chemical species by using gas stream

to blow the plasma out of its production region, thus it is convenient to operate and be employed in practical applications such as surface modification, thin-film deposition, and biomedicine [33-38]. In addition, the plasma jet was investigated in the epoxidation of 1-decene to produce the epoxy products— 1,2-epoxydecane, 1-decanal, 1-nonanal, and 2-decanone [39]. It was hypothesized that a plasma jet could provide a better improvement for ethylene epoxidation performance. Therefore, a cylindrical DBD reactor type was used to redesign a DBD jet reactor for this study.

The main objective of this work was, for the first time, to investigate the ethylene epoxidation in a low-temperature DBD jet system. The separate ethylene/oxygen feed system— ethylene gas stream was directly injected at the end of plasma region while oxygen balanced with argon was fed at the beginning plasma zone to produce oxygen active species— was used to reduce all undesirable other reactions such as cracking and dehydrogenation. The effects of total feed flow rate, oxygen-to-ethylene feed molar ratio, applied voltage, input frequency, and inner electrode position on the epoxidation reaction efficiency in the terms of reactant conversions, EO yield, EO selectivity, and power consumption were examined to obtain that the best conditions for ethylene epoxidation.

7.3 Experimental

7.3.1 Dielectric Barrier Discharge (DBD) Jet System

The configuration of DBD jet reactor and the schematic of experimental setup for ethylene epoxidation reaction are shown in Figure 7.1(a) and (b), respectively. The DBD jet reactor consisted of a quartz tube with 1 cm outer diameter and 10.5 cm length, and two electrodes which made of stainless steel. An outer electrode (high-voltage side) had an inner diameter of 1 cm and a length of 1 cm, whereas an inner electrode (ground side) had a diameter of 1 mm and a length of 17 cm. The gap distance between two electrodes was fixed at 7 mm, except in the case of the effect of inner electrode position.

(a)

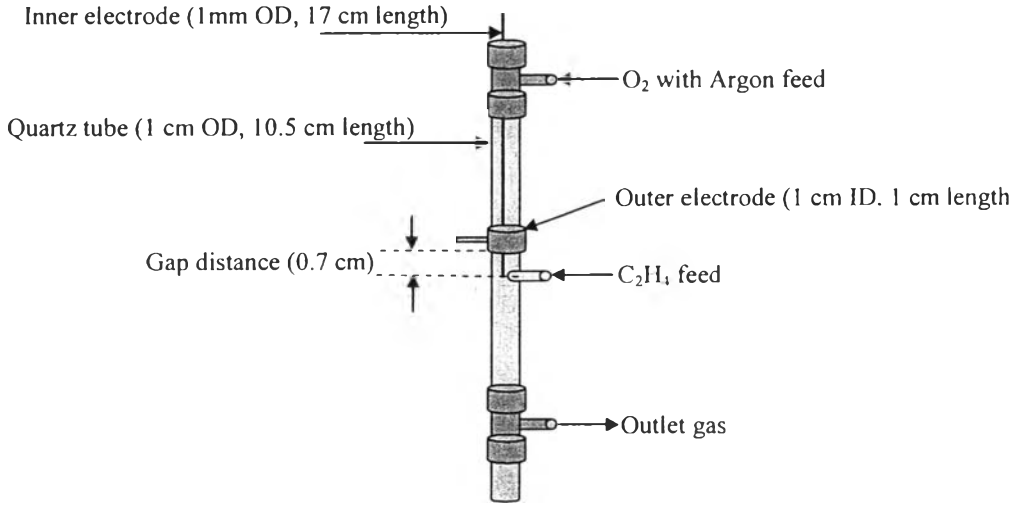

(b)

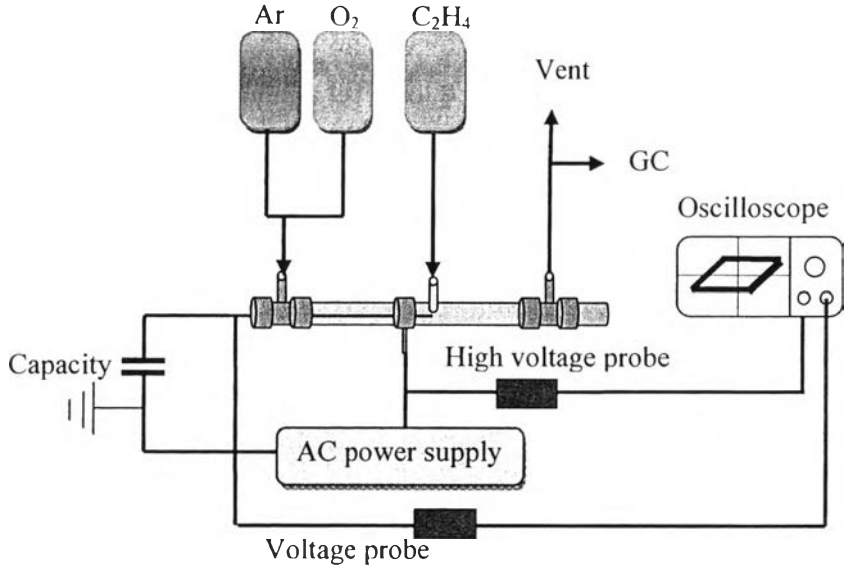

Figure 7.1 (a) Configuration of the DBD jet reactor and (b) Schematic of experimental setup of DBD jet system for ethylene epoxidation reaction.

7.3.2 Reaction Activity Experiments

The C_2H_4 epoxidation reaction was investigated in a DBD jet reactor at ambient temperature (about of 25 °C) and atmospheric pressure. In this study, the flow rates of C_2H_4 and O_2 balanced with argon flowing through the DBD jet reactor as illustrated in Figure 7.1(b) were regulated by rotameters (KOFLOC, accuracy ±2% for C_2H_4, ±1% for O_2, and ±5% for argon). After the compositions of the feed

were invariant with time, a AC generator (Model PM 04015, TREK Inc) was turned on. The voltage and discharge current were monitored by an oscilloscope (TDS3012, Tektronix Inc). After the system reached equilibrium which normally spent 3 min after turning AC generator, product gases were analyzed by a gas chromatograph (SHIMADZU). The gas chromatograph was equipped with both a thermal conductivity detector (TCD) and a flame ionization detector (FID). For the TCD detector (SHIMADZU, GC-8A), a packed column (Molecular sieve 13X) was employed for separating the product gases such as H_2 and O_2 while another column (Parapak Q (2M)) was used to detect CO and CO_2. For the FID detector (SHIMADZU, GC-14B), the column (GS-GasPro) was used for analysis of C_2H_4, ethylene oxide (C_2H_4O, EO), and other product gases, i.e. CH_4, C_2H_2, C_2H_4, C_2H_6, C_3H_6, C_3H_8, n-C_4H_{10}, i-C_4H_{10}, and 1,3-C_4H_{10}.

To evaluate the process performance, the experimental data taken under steady state were averaged (with a standard deviation of less than 5%) and then used to calculate the conversions of ethylene, the selectivities for products, including H_2, EO, CH_4, C_2H_2, C_2H_4, C_2H_6, C_3H_6, C_3H_8, n-C_4H_{10}, i-C_4H_{10}, and 1,3-C_4H_{10}, and the EO yield as following equations:

$$\% \text{ Reactant conversion} = \frac{(\text{moles of reactant in} - \text{moles of reactant out}) \times 100}{(\text{moles of reactant in})} \quad (7.1)$$

$$\% \text{ Product selectivity} = \frac{[(\text{number of carbon atom in product})(\text{moles of product produced})] \times 100}{[(\text{number of carbon atom in } C_2H_4)(\text{moles of } C_2H_4 \text{ converted})]} \quad (7.2)$$

$$\% \text{ EO yield} = \frac{(\% \ C_2H_4 \text{ conversion}) \times (\% \text{ EO selectivity})}{100} \quad (7.3)$$

$$\% \text{ Coke formation} = \frac{([R]C_R - \sum [P_i]C_{Pi}) \times 100}{[R]C_R} \quad (7.4)$$

$$\% \text{ Water formation} = \frac{([R]H_R - \sum [P_i]H_{Pi}) \times 100}{[R]H_R} \quad (7.5)$$

where [P] = moles of product in the outlet gas stream

[R] = moles of C_2H_4 in the feed stream to be converted

C_P = number of carbon atoms in a product molecule

C_R = number of carbon atom in C_2H_4 molecule

H_P = number of H atoms in a product molecule

H_R = number of H atoms in C_2H_4 molecule

To determine the energy efficiency of the plasma system, the electric power, so-called input power, was estimated by Lissajous method [40] and then the power consumption was calculated in a unit of Ws per molecules of C_2H_4 converted or per molecules of EO produced using the following equation:

$$\text{Power consumption} = \frac{P \times 60}{N \times M} \tag{7.6}$$

where P = Power (W)

N = Avogadro's number = 6.02×10^{23} molecules/mol

M = Rate of converted C_2H_4 molecules in feed or rate of produced EO molecules (mol/min).

7.4 Results and Discussion

7.4.1 Effect of Total Feed Flow Rate

To investigate the effect of total feed flow rate on ethylene epoxidation performance under the DBD plasma jet, the total feed flow rate is experimentally varied, as shown in Table 7.1 while an O_2/C_2H_4 feed molar ratio, an input frequency, and an applied voltage are fixed at 0.25, 500 Hz, and 7 kV, respectively.

Table 7.1 Flow rates of three feed gases for each total feed flow rate used in this study

Flow rate (cm^3/min)				Residence time
40% C_2H_4	97% O_2	Argon	Total feed	(s)
100	25	1,500	1,625	0.0229
117	29	1,750	1,896	0.0196
133	33	2,000	2,167	0.0172
150	38	2,250	2,438	0.0153
167	42	2,500	2,708	0.0137
200	50	3,000	3,250	0.0114
233	58	3,500	3,792	0.0099

From the experiments, a total feed flow rate, especially lower than 1,625 cm^3/min, was found to be not sufficient to blow the plasma out, resulting in a very high discharge temperature inside the plasma zone between inner and outer electrodes. This led to the appearance of little flame at the corner of the C_2H_4 feed point and after that discharges extinguished. Therefore, the total feed flow rate of 1,625 cm^3/min was a minimum operationalable flow rate in this study. Figure 7.2(a), shows the effect of total feed flow rate on both C_2H_4 and O_2 conversions. The O_2 conversion significantly decreased over entire total feed flow ranges of 1,625-3,792 cm^3/min, whereas the C_2H_4 conversion gradually decreased with increasing total feed flow rate from 1,625 to 1,896 cm^3/min, then slightly increased with further increasing total feed flow rate to 3,250 cm^3/min, and finally decreased slightly at the highest total feed flow rate of 3,792 cm^3/min. The selectivities for EO and other products and EO yield are showed in Figure 7.2(b) and (c). Small amounts of CH_4, C_2H_6, C_3H_6, C_3H_8, and C_4H_{10} were produced over the entire total feed flow rate range while both C_2H_2 and CO_2 were not produced. The H_2 selectivity, EO selectivity and yield had the same trend with O_2 conversion that decreased with increasing total feed flow rate from 1,625 to 3,792 cm^3/min. This is because an increase in total feed flow rate reduced the contact time of highly active species and energetic electron collisions, leading to reduction of EO and H_2 selectivities, EO yield, O_2 conversion, and C_2H_4 conversion. The generated plasma jet length significantly increased with

increasing total feed flow rate, leading to the enhancement of plasma reaction volume. Hence, the C_2H_4 conversion slightly increased when total feed flow rate increased from 1,896 to 3,250 cm^3/min. However, the DBD jet system under the highest total flow rate (3,792 cm^3/min) seemed to have insufficient contact time for ethylene epoxidation. The C_2H_4 recombination occurred instead, resulting in decreasing C_2H_4 conversion in the total feed flow rate range of 3,250-3,792 cm^3/min. In contrast to EO selectivity, the CO selectivity remained almost unchanged in the total feed flow rate range of 1,625-2,438 cm^3/min but it increased nearly linearly with increasing total feed flow rate beyond the total feed flow rate of 2,438 cm^3/min. The CH_4 selectivity was relatively low and reached zero when the total feed flow rate exceeded 3,250 cm^3/min. The results indicate that the DBD jet system operated at a high total feed flow rate in the range of 2,708-3,792 cm^3/min was more like to promote the combustion or deep oxidation, resulting in lowering EO selectivity.

Figure 7.2(d) illustrates the effect of total feed flow rate on the power consumption per C_2H_4 molecule converted or EO molecule produced. With increasing total feed flow rate, both the power consumptions per C_2H_4 molecule converted and EO molecule produced tended to significantly increase while the current was nearly unchanged over the entire total feed flow rate range (Figure 7.2(e)). Interestingly, the coke and water formation (Figure 7.2 (f)) mirrored the C_2H_4 conversion in the way that they initially decreased at the low total feed flow rate range of 1,625-1,896 cm^3/min, then tended to increase with increasing total feed flow rate from 1,896 to 3,250 cm^3/min, and finally decreased with further increasing total feed flow rate above 3,250 cm^3/min. The results indicate that the system should be operated at low total feed flow rate in order to minimize water formation. From the above mentioned results, a total feed flow rate of 1,625 cm^3/min was considered to be an optimum value when it could provide the highest EO selectivity and yield, and C_2H_4 and O_2 conversions with the lowest power consumption per C_2H_4 molecule converted or EO molecule produced and a relatively low water formation.

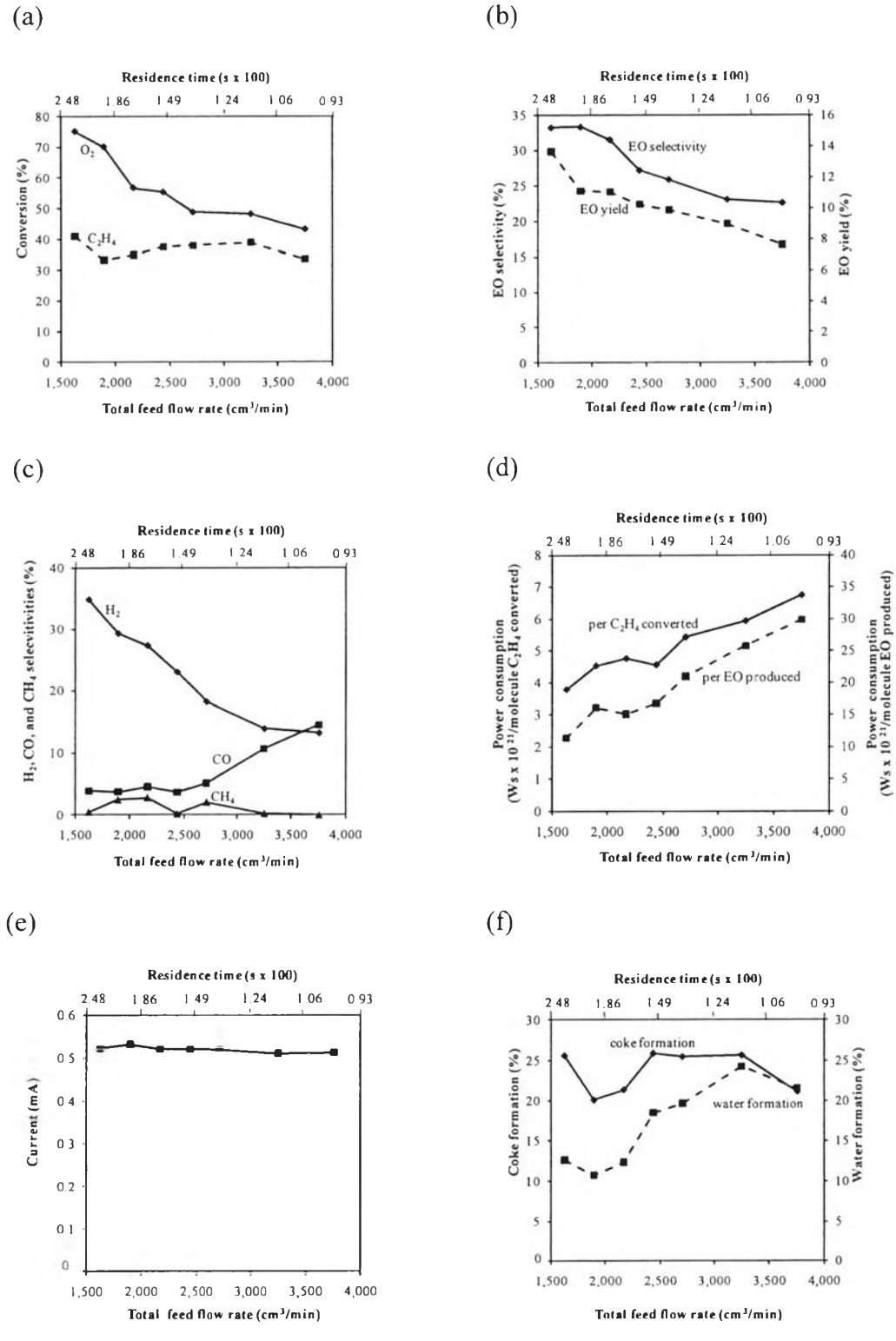

Figure 7.2 (a) C_2H_4 and O_2 conversions, (b) EO selectivity and yield, (c) other product selectivities, (d) power consumption, and (e) coke and water formation as a function of total flow rate (an O_2/C_2H_4 feed molar ratio of 1/4, an applied voltage of 7 kV, and an input frequency of 500 Hz).

7.4.2 Effect of O_2/C_2H_4 Feed Molar Ratio

To study the effect of O_2/C_2H_4 feed molar ratio, the DBD jet system was operated at different O_2/C_2H_4 feed molar ratios of 0.2:1, 0.25:1, 0.3:1, 0.35:1, 0.4:1, and 0.5:1 with a fixed C_2H_4 flow rate of 100 cm^3/min and a total flow rate of 1,625 cm^3/min. As shown in Figure 7.3(a), the O_2 conversion tends to gradually increase with increasing O_2/C_2H_4 feed molar ratio over the entire range of 0.2:1-0.5:1. The C_2H_4 conversion significantly increased when O_2/C_2H_4 feed molar ratio increased from 0.2:1 to 0.3:1, and then it remained almost unchanged with further increasing O_2/C_2H_4 feed molar ratio above 0.3:1. From the results as shown in Figure 7.3(b), the EO selectivity and yield significantly increases when the O_2/C_2H_4 feed molar ratio increases from 0.2:1 to 0.25:1, and then adversely decreases with further increasing O_2/C_2H_4 feed molar ratio from 0.25:1 to 0.4:1. However, when the O_2/C_2H_4 feed molar ratio increased beyond 0.4:1, both EO selectivity and yield slightly increased. The results can be explained by the fact that the studied DBD jet system was operated under the O_2-lean conditions; thus the O_2 is the limiting reactant. However, an increase in O_2/C_2H_4 feed molar ratio beyond 0.3:1 promoted the combustion reaction to form CO more than ethylene epoxidation. From the results, the O_2/C_2H_4 feed molar ratio of 0.25:1 was considered to be an appropriate value for the ethylene epoxidation.

Figure 7.3(c) shows the effect of O_2/C_2H_4 feed molar ratio on selectivities for H_2 and CO, whereas the selectivities of other by-products, i.e. CH_4, C_2H_6, and C_2H_6, are not shown here because of their extremely low values (less than 1% for CH_4 and 0.05% for C_2H_6, and C_2H_6). The H_2 selectivity decreased with increasing O_2/C_2H_4 feed molar ratio from 0.2:1 to 0.3:1, whereas it increased with further increasing O_2/C_2H_4 feed molar ratio beyond 0.3:1. The CO selectivity was found to increase with increasing O_2/C_2H_4 feed molar ratio throughout the entire studied range. The results confirm that high O_2/C_2H_4 feed molar ratios (0.3:1-0.5:1) are not appropriate for the ethylene epoxidation because they prefer the hydrogen formation and hydrocarbon combustion, resulting in increasing H_2 and CO selectivities.

As shown in Figure 7.3(d), the O_2/C_2H_4 feed molar ratio predominantly influenced the power required for the DBD jet system while the current remained

almost unchanged when the O_2/C_2H_4 feed molar ratio increased in the range of 0.2:1-0.3:1. Figure 7.3(e) illustrates the power consumption per C_2H_4 molecule converted or EO molecule produced as a function of O_2/C_2H_4 feed molar ratio. The power consumption per C_2H_4 molecule converted tended to decrease with increasing O_2/C_2H_4 feed molar ratio up to 0.5:1, whereas the power consumption per EO molecule produced rapidly decreased to reach a minimum value at an O_2/C_2H_4 feed molar ratio of 0.25:1, then increased with increasing O_2/C_2H_4 feed molar ratio from 0.25:1 to 0.4:1, and finally decreased with further increasing O_2/C_2H_4 feed molar ratio beyond 0.4:1.

Beside the desired EO, H_2, and CO products, coke and water were produced by the studied DBD jet system. Coke deposited on the inner electrode while water vapor could not be collected to measure the amount of produced water. Therefore, the coke and water formations were computed by carbon and hydrogen balances, as shown on Figure 7.3(f). With increasing O_2/C_2H_4 feed molar ratio from 0.2:1 to 0.3:1, the proportion of available oxygen free radicals increased in the DBD jet system and then caused enhancement of hydrocarbon combustion, resulting in significantly increasing coke and water formations. However, both coke and water formations decreased with further increasing O_2/C_2H_4 feed molar ratio above 0.3:1. This may be possible that an increase in oxygen available in the system simply promotes the formation of CO with less coke formation. Moreover, the DBD jet system under the O_2/C_2H_4 feed molar ratio range of 0.3:1-0.5:1 seemed to prefer H_2 formation reaction rather than water formation. Thus, the H_2 selectivity increased with increasing O_2/C_2H_4 feed molar ratio from 0.3:1 to 0.5:1. From the results, the O_2/C_2H_4 feed molar ratio of 0.25:1 was considered to be an optimum value for ethylene epoxidation because it provided the highest EO selectivity and yield, as well as the lowest H_2 selectivity and power consumption per EO molecule produced.

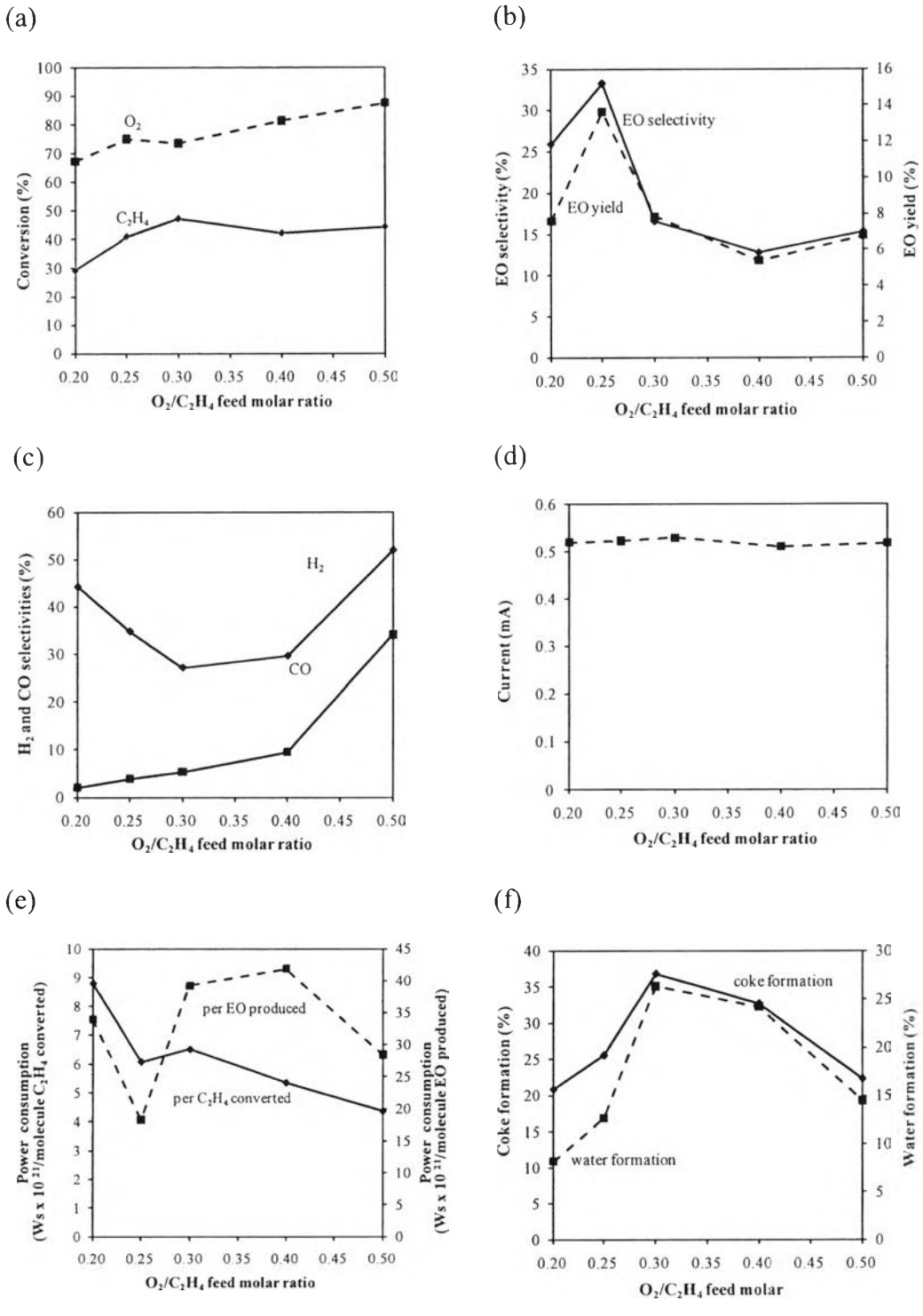

Figure 7.3 (a) C_2H_4 and O_2 conversions, (b) EO selectivity and yield, (c) other product selectivities, (d) input power and discharge current, (e) power consumption, and (f) coke and water formation as a function of O_2/C_2H_4 feed molar ratio (a total flow rate of 1,625 cm^3/min, an applied voltage of 7 kV, and an input frequency of 500 Hz).

7.4.3 Effect of Applied Voltage

From the preliminary results on the voltage range, it was found that the breakdown voltage, or the lowest voltage needed to generate discharges, was about 7 kV, and the discharge was not uniform and stable at a voltage above 15 kV. Therefore, the effect of applied voltage was investigated in the range of 7-15 kV. As shown in Figure 7.4(a), the O_2 conversion gradually increased over the entire applied voltage range of 7-15 kV while the C_2H_4 conversion was almost unchanged. Interestingly, the EO selectivity and yield significantly increased when the applied voltage increased from 7 to 9 kV (Figure 7.4(b)). This is because an increase in the applied voltage increases the generated current and consequently leads to a higher power for production of plasma discharges, as illustrated in Figure 7.4(c). However, both EO selectivity and yield tended to decrease with further increasing applied voltage over 9 kV. The H_2 and CO selectivities significantly increased with increasing applied voltage from 7 to 15 kV, while CH_4 selectivity remained nearly unchanged (Figure 7.4(d)).

The power consumption per C_2H_4 molecule converted or EO molecule produced as a function of the applied voltage is shown in Figure 7.4(e). Both power consumptions had the same trend that they decreased with increasing applied voltage from 7 to 9 kV, and then tended to increase with further increasing applied voltage up to 15 kV. The coke formation slightly decreased when the applied voltage increased from 7 to 9 kV, then gradually increased with increasing applied voltage from 9 to 11 kV, and finally remained almost unchanged with further increasing applied voltage above 11 kV (Figure 7.4(f)). As shown in Figure 7.4(f), the applied voltage shows more influences on the water formation than coke formation. The water formation decreased with increasing applied voltage from 7 to 9 kV, then increased with further increasing applied voltage above 9 kV, and finally it gradually decreased when the applied voltage increased from 9 to 15 kV. It indicated that at the high applied voltage in the range of 9 to 15 kV, the main reactions were the hydrocarbon combustion, H_2 formation, and coke formation instead of ethylene epoxidation. From the results, the applied voltage of 9 kV was an optimum value for ethylene epoxidation and then was employed to further investigate in the effect of the

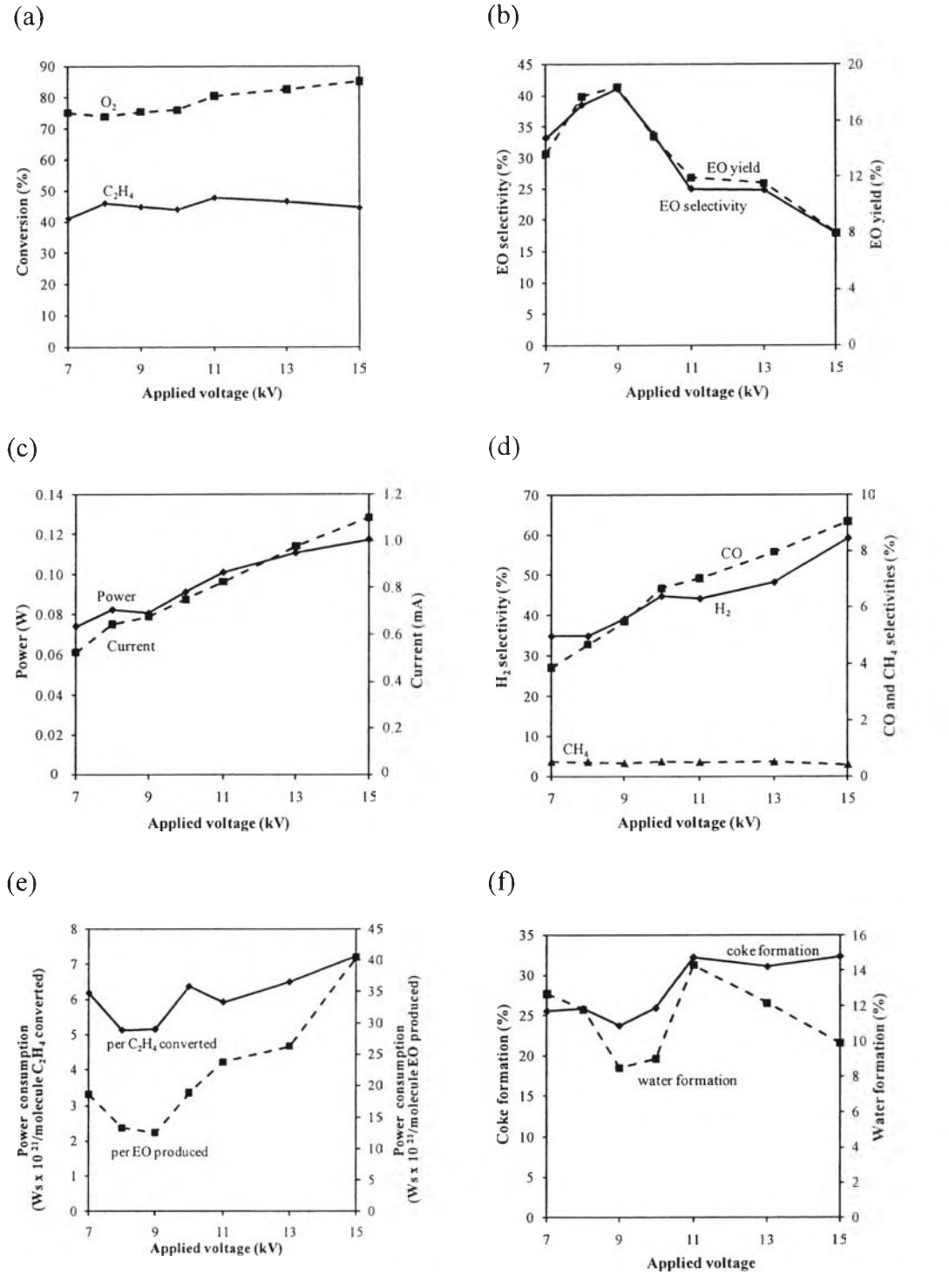

Figure 7.4 (a) C_2H_4 and O_2 conversions, (b) EO selectivity and yield, (c) other product selectivities, (d) input power and discharge current, (e) power consumption, and (f) coke and water formation as a function of applied voltage (a total flow rate of 1,625 cm^3/min, an O_2/C_2H_4 feed molar ratio of 0.25, and an input frequency of 500 Hz).

input frequency because it provided the highest EO selectivity and yield, as well as the lowest power consumption, coke and water formations.

7.4.4 Effect of Input Frequency

The input frequency is an important parameter, directly affecting the field strength in the plasma zone. To investigate the effect of the input frequency on the ethylene epoxidation, the input frequency was varied in the range of 300-900 Hz. The plasma could not exist at the input frequency lower than 300 Hz, while plasma strength was very high intensity at the input frequency higher than 900 Hz, leading to a large amount of coke formation. Figure 7.5(a) shows the effect of input frequency on the C_2H_4 and O_2 conversions. The input frequency significantly affected the O_2 conversion that decreased with increasing input frequency from 300 to 900 Hz, whereas C_2H_4 conversion remained almost unchanged over the entire input frequency range of 300-900 Hz. The EO selectivity and yield had the same trend as O_2 conversion that they decreased with increasing input frequency from 300 to 900 Hz (Figure 7.5(b)). In contrast to EO selectivity, the H_2 selectivity significantly increased with increasing input frequency from 300 to 900 Hz while CO selectivity increased in the input frequency range of 300-800 Hz, and then slightly decreased at high input frequency of 900 Hz (Figure 7.5(c)). The CH_4 selectivity rapidly increased with increasing input frequency from 300 to 500 Hz, and finally tended to decrease with further increasing input frequency.

Figure 7.5(d) illustrates that an increase in the input frequency results in an increase in current and power, required for operating the DBD jet system. In this work, the AC/DC generator was employed to monitor the current, expressing the average current in a second. The current increased with increasing input frequency had the opposite trend, as shown in the previous work [28], because the current in the previous work was based on a discharge, resulting in decreasing current with increasing input frequency. Both power consumptions per C_2H_4 molecule converted and EO molecule produced significantly increased when the input frequency increased, especially from 500 to 900 Hz (Figure 7.5(e)). The coke formation gradually increased over the entire input frequency range of 300-900 Hz, while the water formation initially decreased with increasing input frequency from 300 to 500

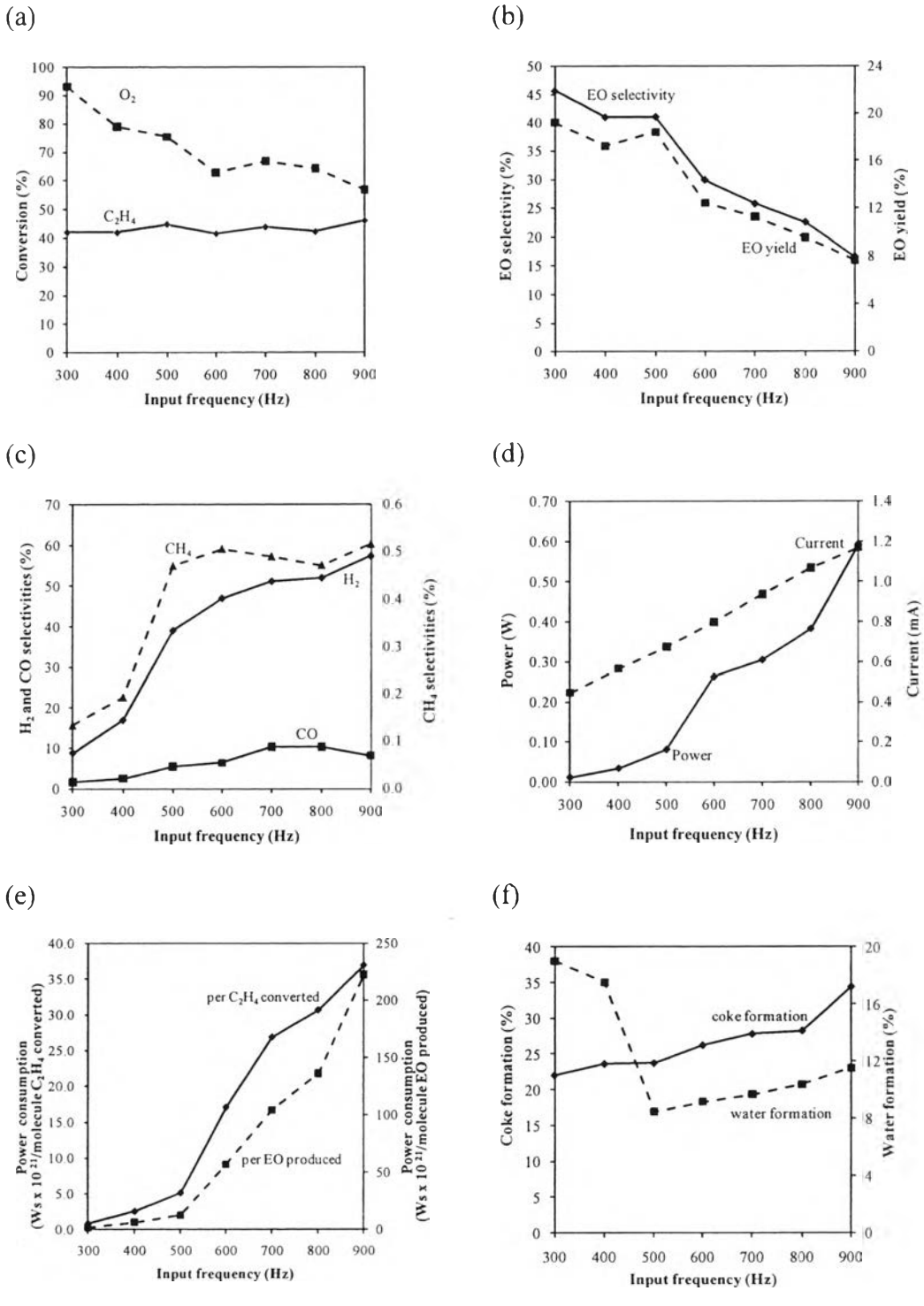

Figure 7.5 (a) C_2H_4 and O_2 conversions, (b) EO selectivity and yield, (c) other product selectivities, (d) input power and discharge current, (e) power consumption, and (f) coke and water formation as a function of applied voltage (a total flow rate of 1,625 cm^3/min, an O_2/C_2H_4 feed molar ratio of 0.25, and an applied voltage of 9 kV).

Hz, and then slightly increased with further increasing input frequency above 500 Hz (Figure 7.5(f)).

From the results, the input frequency of 300 Hz was considered to be an optimum value for ethylene epoxidation because it provided the highest EO selectivity and yield as well as the lowest power consumption, selectivities for H_2, CO, CH_4, and coke formation.

7.4.5 Effect of the Spacing of Inner Pin Electrode and C_2H_4 Feed Point

The effect of the spacing of an inner pin electrode and C_2H_4 feed point on the ethylene epoxidation reaction is shown in Figure 7.6. The spacing of an inner pin electrode and C_2H_4 feed point was defined as a distance between the middle of C_2H_4 feed stream and the tip of the inner pin electrode. The shorter the spacing of an inner pin electrode and C_2H_4 feed point, the higher the opportunity of collision of C_2H_4 molecules with highly energetic electrons and active oxygen species, to yield leading to subsequent reactions, especially deep combustion and H_2 formation. From the results as shown in Figure 7.7(a), the spacing of an inner pin electrode and C_2H_4 feed point greatly affects the C_2H_4 conversion but the O_2 conversion remained almost unchanged. The C_2H_4 conversion increased with increasing spacing of an inner pin electrode and C_2H_4 feed point from 0 to 3 mm, and reached a maximum at the spacing of an inner pin electrode and C_2H_4 feed point of 3 mm. The EO selectivity and yield had the same trend as the C_2H_4 conversion (Figure 7.7(b)). The highest EO selectivity and yield were obtained at the spacing of an inner pin electrode and C_2H_4 feed point of 3 mm whereas the selectivities for H_2, CO, and CH_4 decreased with increasing spacing of an inner pin electrode and C_2H_4 feed point from 0 to 6 mm (Figure 7.7(c)). These results can be explained by the fact that a decrease in spacing of an inner pin electrode and C_2H_4 feed point increases the reaction volume or reaction time, leading to higher opportunity of C_2H_4 cracking and further reactions including H_2 formation and deep combustion. As a consequence, both EO selectivity and yield decreased with decreasing spacing of an inner pin electrode and C_2H_4 feed point. However, the spacing of an inner pin electrode and C_2H_4 feed point of 6 mm was too far from the C_2H_4 feed point in which most generated active oxygen species were recombined before reacting with C_2H_4 molecules, leading to lowering EO

formation. From the results, the spacing of an inner pin electrode and C_2H_4 feed point of 3 mm gave the highest activity toward ethylene epoxidation reaction (Figure 7.6(b)).

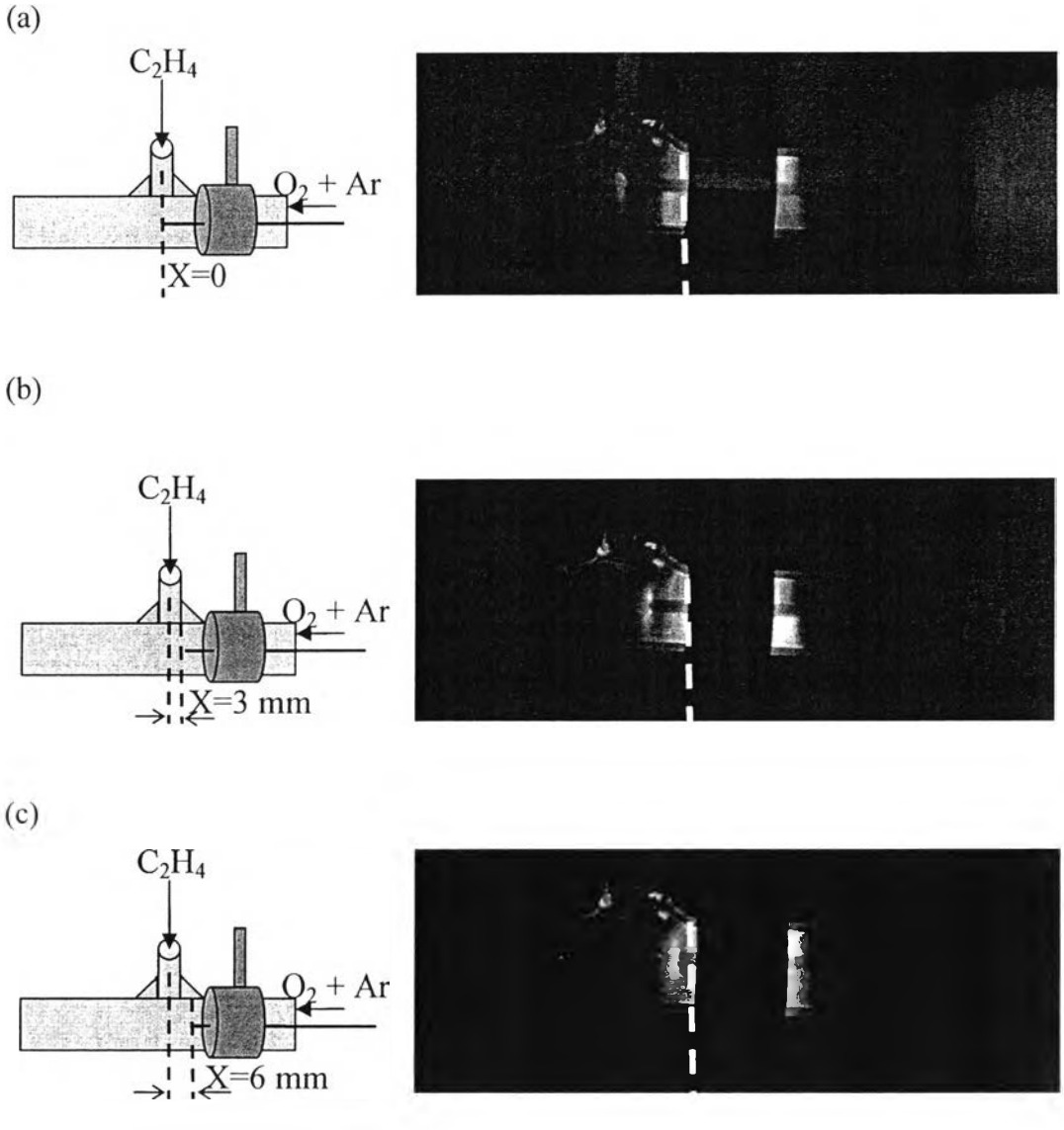

Figure 7.6 Images of generated plasma at different spacing of an inner pin electrode and C_2H_4 feed point: (a) 0 mm, (b) 3 mm, and (c) 6 mm (a total flow rate of 1,625 cm^3/min, an O_2/C_2H_4 feed molar ratio of 0.25, an applied voltage of 9 kV, and an input frequency of 300 Hz).

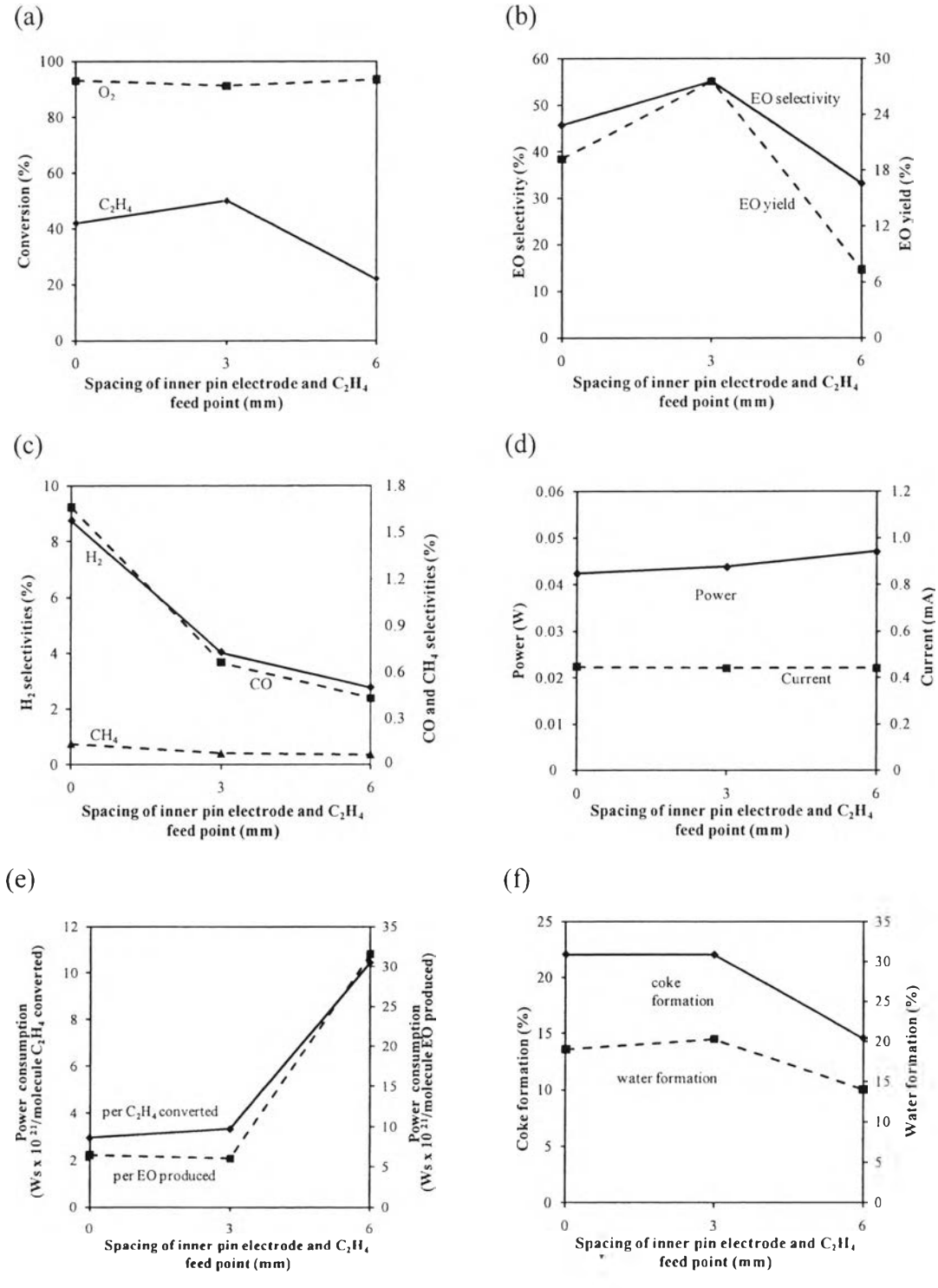

Figure 7.7 (a) C_2H_4 and O_2 conversions, (b) EO selectivity and yield, (c) other product selectivities, (d) input power and discharge current, (e) power consumption, and (f) coke and water formation as a function of inner electrode position (a total flow rate of 1,625 cm^3/min, an O_2/C_2H_4 feed molar ratio of 0.25, an applied voltage of 9 kV, and an input frequency of 500 Hz).

The spacing of an inner pin electrode and C_2H_4 feed point slightly influences the generated current and consumed power, as shown in Figure 7.7(d), while the power consumption per C_2H_4 molecule converted or EO molecule produced slightly varies in the range of the spacing of an inner pin electrode and C_2H_4 feed point of 0-3 mm, and then rapidly rises up with further increasing spacing of an inner pin electrode and C_2H_4 feed point above 3 mm, as shown in Figure 7.7(e). As shown in Figure 7.7(f), the coke and water formations remain almost unchanged in the range of the spacing of an inner pin electrode and C_2H_4 feed point of 0-3 mm, and then decreased with further increasing from 3 to 6 mm. For the results, the spacing of an inner pin electrode and C_2H_4 feed point of 3 mm was considered to be an optimum value for ethylene epoxidation because it gave the highest EO selectivity and yield as well as the lowest power consumption.

7.5 Conclusions

In this work, the epoxidation of ethylene was investigated in a low-temperature DBD jet system. A high flow rate with O_2-lean conditions was needed to form the plasma jet. The C_2H_4 stream was separately injected at the end of the plasma zone in order to reduce C_2H_4 cracking and further reactions, while the O_2 balanced with argon was thoroughly fed into a DBD jet reactor. The DBD jet provided obviously high potential for ethylene epoxidation with very low power consumption. For further study, active catalysts are interesting to apply in the DBD jet system for solving the coke formation. The highest EO selectivity and yield, as well as the lowest power consumption were obtained at a total feed flow rate of 1,625 cm^3/min, an O_2/C_2H_4 feed molar ratio of 0.25:1, an applied voltage of 9 kV, an input frequency of 300 Hz, and an inner electrode position of 0.3 mm.

7.6 Acknowledgements

The authors would like to gratefully acknowledge Dudsadeepipat Scholarship, Chulalongkorn University, Thailand; the Research Unit of Petrochemical and Environmental Catalysis under the Ratchadapisek Somphot

Endowment Fund, Chulalongkorn University, Thailand; and Excellence Center on Petrochemical, and Materials technology, Chulalongkorn University, Thailand.

7.7 References

1. http://www.osha.gov/OshDoc/data_General_Facts/ethylene-oxide-factsheet.pdf (accessed on February 6, 2011)
2. http://www.epa.gov/ttn/atw/hlthef/ethylene.html (accessed on February 6, 2011)
3. Tan SA, Grant RB, Lambert RM (1987) Appl Catal 31:159
4. Jun Y, Jingfa D, Xiaohong Y, Shi Z (1992) Appl Catal A: Gen 92:73
5. Goncharova SN, Paukshtis EA, Bal'zhinimaev BS (1995) Appl Catal A: Gen 126:67
6. Macleod N, Keel JM, Lambert RM (2003) Catal. Lett. 86:51
7. Ayame A, Uchida Y, Ono H, Miyamoto M, Sato T, Hayasaka H (2003) Appl Catal A: Gen 244:59
8. Linic S, Barteau MA (2004) J Am Chem Soc 126:8086
9. Jankowick JT, Barteau MA (2005) J Catal 236:366
10. Jankowick JT, Barteau MA (2005) J Catal 236:379
11. Dellamorte JC, Lauterbach J, Barteau MA (2007) Catal today 120:182
12. Rojluechai S, Chavadej S, Schwank JW, Meeyoo V (2007) Catal Comun 8:57
13. Piccinin S, Nguyen NL, Stampfl C, Scheffler M (2010) J Mater Chem 20:10521
14. Tan SA, Grant RB, Lambert RM (1987) J Catal 106:54
15. Torres D, Illas F, Lambert RM (2008) J Catal 260:380
16. Ozbek MO, Onal I, Van Santen RA (2011) J Phys: Condens Matter 23: art no 404202
17. Yang Y (2003) Plasma Chem Plasma Process 23:283 Jun
18. Mizeraczyk J, Jasiński M, Zakrzewski Z (2005) Plasma Phys Controlled Fusion 47: B589-B602
19. Kodama S, Sekiguchi H (2006) Thin Solid Films 506-507:327
20. Lazaroiu Gh, Zissulescu E, Sandu M, Roscia M (2007) Energy 32:2412 Dec
21. De Geyter N, Morent R, Jacobs T, Axisa F, Gengembre L, Leys C, Vanfleteren J, Payen E (2009) Plasma Process Polym 6: S406-S411

22. Vinogradov I, Lunk A (2009) Plasma Process Polym 6: S514-S518

23. Yaghmaee MS, Shokri B, Khiabani NH, Sarani A (2009) Plasma Process Polym 6: S631-S636

24. Thevenet F, Couble J, Brandhorst M, Dubois JL, Puzenat E, Guillard C, Bianchi D (2010) Plasma Chem Plasma Process 30:489 Aug

25. Leduc M, Guay D, Coulombe S, Leask RL (2010) Plasma Process Polym 7:899 Nov

26. Rosacha LA, Anderson GK, Bechtold LA, Coogan JJ, Heck HG, Kang M, McCulla WH, Tennant RA, Wantuck PJ, NATO ASI series (1993) 34, part B.

27. Suhr H, Schmid H, Pfeundschuh H, Lacocca D (1984) Plasma Chem Plasma Process 4:285

28. Chavadej S, Tansuwan A, Sreethawong T (2008) Plasma Chem Plasma Process 28:643

29. Sreethawong T, Suwannabart T, Chavadej S (2009) Chem Eng J 115:396

30. Sreethawong T, Suwannabart T, Chavadej S (2008) Plasma Chem Plasma Process 28:629

31. Sreethawong T, Permsin N, Suttikul T, Chavadej S (2010) Plasma Chem Plasma Process 30:503

32. Lei X, Fang Z (2011) IEEE T Plasma Sci 39:2288

33. Panousis E, Clément F, Loiseau JF, Spyrou N, Held B, Larrieu J, Lecoq E, Guimon C (2007) Surf Coat Tech 201:7292

34. Guimin X, Guanjun Z, Xingmin S, Yue M, Ning W, Yuan L (2009) Plasma Sci Tech 11:83

35. Merche D, Poleunis C, Bertrand P, Sferrazza M , Reniers F (2009) IEEE T Plasma Sci 37:951

36. Chiang MH, Liao KC, Lin IM, Lu CC, Huang HY, Kuo CL, Wu JS (2010) IEEE T Plasma Sci 38:1489

37. Pulpytel J, Kumar V, Peng P, Micheli V, Laidani N, Arefi-Khonsari F (2011) Plasma Process Polym 8:664

38. Shao XJ, Zhang GJ, Zhan JY, Xu GM (2011) IEEE T Plasma Sci 39:3095

39. Yoshinori S, Hidetoshi S (2006) Thin Solid Films 506-507:427

40. Wagner HE, Brandenburg R, Kozlov KV, Sonnenfeld A, Michel P, Behnke JF, (2003) Surf Eng Surf Instrumentation & Vacuum tech 71:417